Publisher: GSA
Journal: GEOL: Geology
DOI:10.1130/G45514.1

Manuscript accepted by ***Geology***. The final publication is available via
https://pubs.geoscienceworld.org/gsa/geology/article-abstract/47/2/123/567988/widespread-seismic-anisotropy-in-earth-s-lowermost?redirectedFrom=fulltext

Widespread seismic anisotropy in Earth’s lowermost mantle beneath the Atlantic and Siberia

Michael Grund and Joachim R. R. Ritter

Geophysical Institute, Karlsruhe Institute of Technology (KIT), Hertzstr. 16, 76187 Karlsruhe, Germany

ABSTRACT

Deep inside the Earth, just above the core-mantle boundary at around 2,700 km depth, large-scale mantle structures are assumed to play a key role for global geodynamic processes. While unusual hot regions are attributed to feed rising mantle plumes and volcanic hotspots, the accumulation of subducted lithospheric plates is associated with colder than average features. In both environments the appearance of dynamic-driven processes such as deformation and mantle flow can directly be inferred by the presence of seismic anisotropy. However, the geometries as well as the interactions of these massive anomalous structures with the surrounding mantle material are still under debate. Based on new seismic data from a dense and large-aperture recording network in Scandinavia we characterize the anisotropic signatures of two so far unexplored regions in the lowermost mantle by using observations of clearly discrepant SKS-SKKS shear wave splitting measurements. Thereby we can demonstrate that anisotropy is located along the

northern edges of the Large Low Shear Velocity Province beneath Africa. Furthermore, we recover an anisotropic structure in a region of fast seismic velocity underneath Siberia which provides additional evidence for widespread deformation caused by a deeply subducted slab.

INTRODUCTION

Teleseismic core-refracted shear waves such as SKS and SKKS sample nearly the same volumes in the upper 500 km of the Earth's mantle for the same source-receiver pair. In contrast, their raypaths differ significantly in the lower mantle (Fig. 1). With the exception of the 200–300 km-thick D″ layer just atop the core-mantle boundary (CMB) the lower mantle is generally assumed to be nearly isotropic (e.g., Meade et al., 1995). Therefore, distinct discrepancies in SKS-SKKS shear wave splitting are a powerful tool to map depth-dependent anisotropic anomalies in D″ (e.g., Lynner and Long, 2014). Recently the observations of discrepant SKS-SKKS splitting pairs increased, especially for areas along the edges of the Large Low Shear Velocity Provinces (LLSVPs) beneath Africa and the Pacific (e.g., Niu and Perez, 2004; Lynner and Long, 2014; Deng et al., 2017) or for more meso-scale structures like the Perm Anomaly beneath Russia (Long and Lynner, 2015). It was inferred that variations of complex and strong anisotropy are located near the boundaries of LLSVPs which are potentially associated with deformation due to mantle flow (e.g., Cottaar and Romanowicz, 2013). Furthermore, there is evidence from SKS-SKKS splitting for anisotropy in D″ caused by remnants of paleo-subducted slab material that induces high shear deformation atop the CMB (e.g., Long, 2009).

Here we present striking new observations of discrepant SKS-SKKS splitting pairs that were recorded across a large-aperture seismic network in Scandinavia and surrounding countries. With our findings we can shed light on two widespread and so far poorly sampled or fully unexplored anomalous regions in D″ that are located along the northern edges of the African LLSVP and beneath northwestern Siberia in an area of consistent fast seismic shear wave velocity (v_S). The knowledge on such anomalies provides rare constraints for improved modeling and understanding of mantle dynamics.

DATA AND METHODS

We analyzed seismic data of more than 250 temporary and permanent stations (Fig. 1) that are mainly part of the ScanArray network (Thybo et al., 2012; Grund et al., 2017). Earthquakes with M_W > 5.8 at distances of 80°-140° were selected for the routine shear wave splitting analysis. Here we only focus on a subset of the whole analyzed data set, namely events for which it was possbile to identify both clear SKS and SKKS arrivals on the same seismogram (Table DR1 in the GSA Data Repository[1]). Shear wave splitting (fast axis ϕ and delay time δt) was measured with the SplitLab package (Wüstefeld et al., 2008), using simultaneously the rotation correlation method (RC, Bowman and Ando, 1987) and the energy minimization method (SC, Silver and Chan, 1991). Prior to the measurements we checked the sensor orientations (see Data Repository for details) and processed the waveforms using a zero-phase bandpass filter (5–15 s). For some recordings the corner periods were slightly adjusted to improve the signal-to-noise ratio (SNR) as done in previous studies (e.g., Long, 2009; Grund, 2017). We only consider measurements that agreed for both methods (RC and SC) within their error bounds (95% confidence region) and which have an SNR ≥ 5. All splitting measurements (Table DR1) have typical errors of less than ± 25° for ϕ (average: ± 15.5°) and ± 0.5 s for δt (±0.32 s). For error estimation we applied the corrected equations by

Walsh et al. (2013) as implemented in the StackSplit plugin (Grund, 2017). Phase arrivals with a clear signal on the radial component, SNR ≥ 5 and (nearly) linear particle motion before the correction for splitting were classified as so-called nulls (no splitting). In our data set we classified a pair of SKS-SKKS as discrepant if one phase was null and the other phase was clearly split. If both phases were split (similar ϕ and δt) or both were null, the pair was considered as non-discrepant (e.g., Long and Lynner, 2015). In order to characterize contributions from lowermost mantle (LMM) anisotropy at stations with complex splitting characteristics (Fig. DR2), we followed the approach of Deng et al. (2017) by measuring the splitting intensity (SI) as decribed by Chevrot (2000). Based on this approach null arrivals in our data set have to fulfill the condition of an absolute SI value that is < 0.2 and for a discrepant SKS-SKKS pair the absolute SI-difference (ΔSI) including the errors has to be ≥ 0.2. For a potential contribution from LMM-anisotropy, ΔSI between SKS and SKKS is expected to be at least ≥ 0.4 (Deng et al., 2017).

RESULTS AND DISCUSSION

Observation of Clearly Discrepant SKS-SKKS Waveforms

Using shear wave splitting analysis, in total we received 332 pronounced SKS-SKKS pairs. (Table DR1). Out of these, 49 pairs show clear discrepancies and 283 pairs offer no anomalous pattern. Figure 2 presents a waveform example of a discrepant SKS-SKKS pair. Further recordings are shown in Figure DR3. If possible we cross-checked the SKS results by measuring splitting also for sSKS. Both phases sample nearly the same volumes along their raypaths and, as expected, the splitting parameters reveal consistency within the limits of uncertainty (Fig. DR4).

Publisher: GSA
Journal: GEOL: Geology
DOI:10.1130/G45514.1

Taking into account finite frequency effects (e.g., Favier and Chevrot, 2003), it is quite unlikely that such waveform discrepancies originate only from shallow anisotropy directly beneath the station. With dominant periods of 6–10 s, the Fresnel zones for SKS and SKKS overlap significantly in the mantle transition zone and uppermost lower mantle (Fig. DR5). For this reason both phases of a pair are sensitive to the same volume and we would expect the same ϕ-δt characteristics. Furthermore, we rule out major influences due to waveform interference between phases arriving at the stations within short time periods (Lin et al., 2014). The observed discrepancies occur for distances of 100°-130° and event depths > 20 km (Fig. DR6). This was assumed to be sufficient to avoid dominant interference effects (Deng et al., 2017) (Figs. DR7, DR8). Hence, our observed SKS-SKKS discrepancies are first-order indicators that a component of LMM-anisotropy plays a key role in this context. However, for observations of non-discrepant pairs (Fig. DR4) a contribution of LMM-anisotropy cannot necessarily be ruled out (e.g., Long and Lynner, 2015). Depending on the raypaths and the dimension of an anomaly with consistent anisotropic properties (ϕ, δt), both phases could be equally split or not split (Fig. DR9).

In order to detect any geographical correlation between the splitting discrepancies and large-scale LMM features, we summarize our results in Figure 3 along with the GyPSuM global v_S tomography model (Simmons et al., 2010) and the pierce points of the SKS-SKKS raypaths in 2,700 km depth. Due to contributions from shallower anisotropy in the upper mantle, at most stations in our network the splitting pattern is not well-constrained or it indicates a non-simple nature of anisotropy (Fig. DR2). Thus, we explicitly cannot correct for likely upper mantle contributions here as done in previous studies with more simple splitting characteristics (e.g., Lynner and Long, 2014). Nevertheless, the evaluation of measured ΔSI allows to explore potential contributions of LMM-anisotropy to the overall splitting signals (Deng et al., 2017).

Geographic Clusters in the Lowermost Mantle

From the locations of the D″ pierce points, the anomalous pairs can be divided into a western and eastern region relative to our station network (Fig. 3). As observed in previous SKS-SKKS studies, the pierce points of discrepant pairs are interleaved by non-discrepant ones that are mostly null/null observations (especially for phase arrivals from west). A possible explanation is that small-scale heterogeneity of anisotropic structure is located along the slightly varying raypaths in the LMM (e.g., Long and Lynner, 2015).

For the eastern region we observe two types of discrepant splitting pairs. First, a set of 22 pairs with split SKKS phases and clear nulls for SKS. The split SKKS phases sample the LMM roughly along an east-west transect (65°N, 60°-92°E) near the edges of a major fast-v_S anomaly in D″ beneath northwestern Siberia (Fig. 3). Besides nearly consistent orientations for ϕ (average 5.3°), ΔSI is > 0.4 for the majority of pairs (Fig. DR10). Moreover, these pairs were recorded at stations that are located on different geological units from southwest Sweden up to northern Finland (Figs. DR7-DR8, DR11). Therefore, such a consistent splitting pattern indicates a large-scale feature of uniform LMM-anisotropy beneath northwestern Siberia that is observed independently from structures directly underneath the network. In contrast, the second group in the east consists of six pairs with split SKS and nulls for SKKS. Beyond that, the orientations for ϕ with nearly east-west alignments differ significantly compared to the first group. The SKS pierce points in D″ are located within a narrow north-south swath (60°-72°N, 45°E)

Publisher: GSA
Journal: GEOL: Geology
DOI:10.1130/G45514.1

that encompasses areas with strong variations in v_S. The two split SKS phases in the south fall into a region of anomalously low v_S that is known as Perm Anomaly (Fig. 3).

Within the western cluster most pierce points of the split SKKS phases cover a nearly north-south oriented area in the LMM beneath the Atlantic west of UK and northwest of France. For the orientations of ϕ (only split SKKS) we also determined consistent directions (average of 39°) whereas δt varies with values ranging from 0.7 s up to 2.1 s. As for the eastern cluster, there is evidence for a contribution from LMM-anisotropy by taking ΔSI into account, with values mostly > 0.4 (Fig. DR10). Most non-discrepant pairs show clear nulls for both phases. A considerable amount of the corresponding pierce points is located close to or within the slow-v_S anomaly beneath Iceland.

Nature of Anisotropy Below Siberia

Below Siberia several global tomography models (including GyPSuM) agree in terms of relatively fast v_S (Shephard et al., 2017, Fig. DR12). This anomaly was interpreted as a remnant of paleosubducted slab material that is reaching down to the CMB (Van der Voo et al., 1999). This hypothesis is supported by previous (source- and receiver-side corrected) S-ScS splitting that revealed a dipping symmetry axis for the anisotropic fabric in a neighboring area (Wookey and Kendall, 2008). Furthermore, in a common geographical reference frame, the estimated orientation for ϕ is similar to ours for a nearly east-west raypath (Fig. DR10). From geodynamic modeling it has been shown that sinking slab material can imprint strong strain-induced anisotropy at the base of the lower mantle (e.g., McNamara et al., 2002). Such a scenario is mainly controlled by the lattice-preferred orientation (LPO) of lower-mantle minerals like post-perovskite (e.g., Merkel et al., 2007). Therefore, we infer that our discrepant SKS-SKKS observations indicate a widespread, so far unsampled region of coherent LPO-induced anisotropy in D″, caused by downwelling slab material that impinges on the CMB beneath Siberia (Fig. 4).

However, so far we cannot fully constrain the geometry of the anisotropic region due to limited ray coverage (except for events from the South Pacific area) and the observed ϕ-δt variations at most of our stations (Fig. DR2). Moreover, it remains unclear whether a change in the geometry or the mechanism of anisotropy is responsible for the significant difference in ϕ between the split SKS and SKKS phases. Nevertheless, based on significant ΔSI (Fig. DR10), we can demonstrate that a component of LMM-anisotropy contributes to the overall splitting signal.

Anisotropic Source Beneath the Atlantic

Different global tomography models (including GyPSuM) consistently have anomalously low v_S and strong lateral velocity gradients from fast to slow seismic velocities along the northern edges of the African LLSVP beneath the Atlantic (Lekic et al., 2012, Fig. DR13). Beyond that, for some models also a potential connection between the African LLSVP and a 250-650 km-wide region of heavily reduced v_S (~ -6% to -10%, Fig. DR10) in D″ below Iceland is detectable (e.g., He et al., 2015) which is located in the so far poorly sampled area of our 19 split SKKS observations up to ~ 50°N (Fig. 3). These splitting observations are in good agreement with previous studies, suggesting strong and complex anisotropy along the edges of LLSVPs and meso-scale structures of similar character (e.g., Long and Lynner, 2015; Deng et al., 2017). In general, this anisotropy is assumed to be induced by complex mantle flow toward the boundaries of the low-v_S zones (e.g., Cottaar and Romanowicz, 2013). The absence of splitting within this zones, however, may indicate vertical mantle flow that feeds the upwelling hot mantle plume beneath Iceland (Fig. 4, He et al., 2015). Taking into account the overall splitting pattern at our long-running permanent stations (Fig. DR2), for most SKS phases from South American earthquakes we received clear nulls indicating no contributions from upper mantle anisotropy for these raypaths. In contrast, the SKKS phases of the same events exhibit consistent splitting with nearly the same orientation for ϕ. Such a scenario allows us to suppose that the orientation of ϕ (measured at the stations), mirrors the true direction of the anisotropy fast axis in the LMM without further influence from the upper mantle. Therefore our striking observations of mainly $\Delta SI > 0.4$ in this area (Fig. DR10) support the idea that anisotropy is also located along the edges of the northern extensions of the African LLSVP towards the low-v_S anomaly beneath Iceland.

CONCLUSIONS

Benefiting from a dense and large-aperture recording network in Scandinavia, we are able to explore two widespread areas on the fragmentary global map of LMM-anisotropy beneath the Atlantic and northwestern Siberia. While previous studies sampled several smaller partly overlapping patches of the LMM, with our observations of clearly discrepant SKS-SKKS splitting pairs we can draw a more complete picture of the whole area (Fig. DR14) although the geometry and mechanism of the anisotropic D″ fabrics cannot be fully derived from our results alone. Nevertheless, this demonstrates that the ongoing deployment of dense and large-aperture seismic networks not only helps to understand the anisotropic structure directly beneath a station itself but can also reveal valuable and poorly needed information about extensive and dynamically active regions in D″ relatively far away from the receiver.

ACKNOWLEDGMENTS

This work has received funding from DFG (Deutsche Forschungsgemeinschaft) via LITHOS-CAPP (RI1133/11–1 and –2). Seismic data were obtained from the data centers GEOFON, Orfeus, IRIS and SEIS-UK as well as Univ. of Helsinki and the Swedish National Seismic Network (SNSN). Devices for the German contribution to ScanArray were provided by the GFZ GIPP instrument pool. Maps were prepared using GMT (Wessel et al., 2013). Abundant helpful comments on the manuscript by T. Hertweck and three anonymous reviewers are acknowledged.

REFERENCES CITED

Bowman, J., and Ando, M., 1987, Shear-wave splitting in the upper-mantle wedge above the Tonga subduction zone: Geophysical Journal of the Royal Astronomical Society, v. 88, p. 25–41, https://doi.org/10.1111/j.1365-246X.1987.tb01367.x.

Chevrot, S., 2000, Multichannel analysis of shear wave splitting: Journal of Geophysical Research, v. 105, p. 21,579–21,590, https://doi.org/10.1029/2000JB900199.

Cottaar, S., and Romanowicz, B., 2013, Observations of changing anisotropy across the southern margin of the African LLSVP: Geophysical Journal International, v. 195, p. 1184–1195, https://doi.org/10.1093/gji/ggt285.

Crotwell, H.P., Owens, T.J., and Ritsema, J., 1999, The TauP toolkit: Flexible seismic travel-time and ray-path utilities: Seismological Research Letters, v. 70, p. 154–160, https://doi.org/10.1785/gssrl.70.2.154.

Deng, J., Long, M.D., Creasy, N., Wagner, L., Beck, S., Zandt, G., Tavera, H., and Minaya, E., 2017, Lowermost mantle anisotropy near the eastern edge of the Pacific LLSVP: Constraints from SKS-SKKS splitting intensity measurements: Geophysical Journal International, v. 210, p. 774–786, https://doi.org/10.1093/gji/ggx190.

Favier, N., and Chevrot, S., 2003, Sensitivity kernels for shear wave splitting in transverse isotropic media: Geophysical Journal International, v. 153, p. 213–228, https://doi.org/10.1046/j.1365-246X.2003.01894.x.

Grund, M., 2017, StackSplit - a plugin for multi-event shear wave splitting analyses in SplitLab: Computers & Geosciences, v. 105, p. 43–50, https://doi.org/10.1016/j.cageo.2017.04.015.

Grund, M., Mauerberger, A., Ritter, J.R.R., and Tilmann, F., 2017, Broadband Recordings for LITHOS-CAPP: LITHOspheric Structure of Caledonian, Archaean and Proterozoic Provinces Sep. 2014 - Oct. 2016, Sweden and Finland, STR-Data 17/02, GIPP Experiment and Data Archive, Potsdam: GFZ German Research Centre for Geosciences, https://doi.org/10.2312/GFZ.b103-17029.

He, Y., Wen, L., Capdeville, Y., and Zhao, L., 2015, Seismic evidence for an Iceland thermo-chemical plume in the Earth’s lowermost mantle: Earth and Planetary Science Letters, v. 417, p. 19–27, https://doi.org/10.1016/j.epsl.2015.02.028.

Lekic, V., Cottaar, S., Dziewonski, A., and Romanowicz, B., 2012, Cluster analysis of global lower mantle tomography: A new class of structure and implications for chemical heterogeneity: Earth and Planetary Science Letters, v. 357–358, p. 68–77, https://doi.org/10.1016/j.epsl.2012.09.014.

Lin, Y.-P., Zhao, L., and Hung, S.-H., 2014, Full-wave effects on shear wave splitting: Geophysical Research Letters, v. 41, p. 799–804, https://doi.org/10.1002/2013GL058742.

Long, M.D., 2009, Complex anisotropy in D″ beneath the eastern Pacific from SKS-SKKS splitting discrepancies: Earth and Planetary Science Letters, v. 283, p. 181–189, https://doi.org/10.1016/j.epsl.2009.04.019.

Long, M.D., and Lynner, C., 2015, Seismic anisotropy in the lowermost mantle near the Perm Anomaly: Geophysical Research Letters, v. 42, p. 7073–7080, https://doi.org/10.1002/2015GL065506.

Lynner, C., and Long, M.D., 2014, Lowermost mantle anisotropy and deformation along the boundary of the African LLSVP: Geophysical Research Letters, v. 41, p. 3447–3454, doi:https://doi.org/10.1002/2014GL059875.

McNamara, A.K., van Keken, P.E., and Karato, S.-I., 2002, Development of anisotropic structure in the Earth's lower mantle by solid-state convection: Nature, v. 416, p. 310–314, https://doi.org/10.1038/416310a.

Meade, C., Silver, P.G., and Kaneshima, S., 1995, Laboratory and seismological observations of lower mantle isotropy: Geophysical Research Letters, v. 22, p. 1293–1296, https://doi.org/10.1029/95GL01091.

Merkel, S., McNamara, A.K., Kubo, A., Speziale, S., Miyagi, L., Meng, Y., Duffy, T.S., and Wenk, H.-R., 2007, Deformation of (Mg,Fe)SiO_3 post-perovskite and D″ anisotropy: Science, v. 316, p. 1729–1732, https://doi.org/10.1126/science.1140609.

Niu, F., and Perez, A.M., 2004, Seismic anisotropy in the lower mantle: A comparison of waveform splitting of SKS and SKKS: Geophysical Research Letters, v. 31, p. L24612, https://doi.org/10.1029/2004GL021196.

Shephard, G.E., Matthews, K.J., Hosseini, K., and Domeier, M., 2017, On the consistency of seismically imaged lower mantle slabs: Scientific Reports, v. 7, p. 10976, https://doi.org/10.1038/s41598-017-11039-w.

Silver, P.G., and Chan, W.W., 1991, Shear wave splitting and subcontinental mantle deformation: Journal of Geophysical Research, v. 96, p. 16429–16454, https://doi.org/10.1029/91JB00899.

Simmons, N.A., Forte, A., Boschi, L., and Grand, S., 2010, GyPSuM: A joint tomographic model of mantle density and seismic wave speeds: Geophysical Research Letters, v. 115, B12310, https://doi.org/10.1029/2010JB007631.

Thybo, H., Balling, N., Maupin, V., Ritter, J., and Tilmann, F., 2012, ScanArray Core (1G 2012–2017): The ScanArray consortium, Other/Seismic Network, http://doi.org/10.14470/6T569239.

Van der Voo, R., Spakman, W., and Bijwaard, H., 1999, Mesozoic subducted slabs under Siberia: Nature, v. 397, p. 246–249, https://doi.org/10.1038/16686.

Walsh, E., Arnold, R., and Savage, M.K., 2013, Silver and Chan revisited: Journal of Geophysical Research, v. 118, p. 5500–5515.

Wessel, P., Smith, W.H.F., Scharroo, R., Luis, J., and Wobbe, F., 2013, Generic Mapping Tools: Improved version released: Eos Transactions, American Geophysical Union, v. 94, p. 409–420.

Wookey, J., and Kendall, J.-M., 2008, Constraints on lowermost mantle mineralogy and fabric beneath Siberia from seismic anisotropy: Earth and Planetary Science Letters, v. 275, p. 32–42, https://doi.org/10.1016/j.epsl.2008.07.049.

Wüstefeld, A., Bokelmann, G., Zaroli, C., and Barruol, G., 2008, SplitLab: A shear-wave splitting environment in Matlab: Computers & Geosciences, v. 34, p. 515–528, https://doi.org/10.1016/j.cageo.2007.08.002.

FIGURES AND CAPTIONS

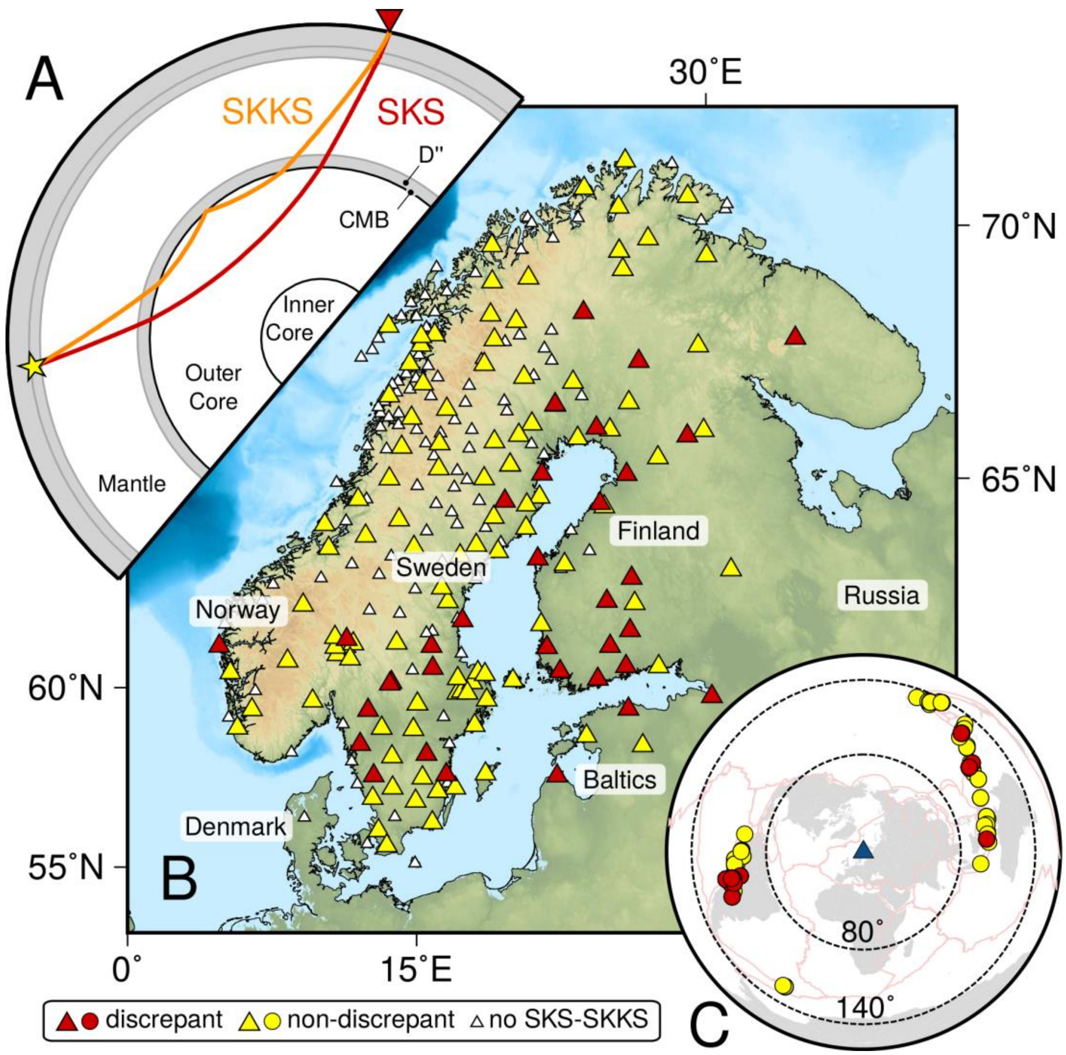

Publisher: GSA
Journal: GEOL: Geology
DOI:10.1130/G45514.1

Figure 1. A: SKS-SKKS raypaths from hypocenter (star) to receiver (500 km depth, Δ ~100°). B: Seismic stations used in this study (triangles). Color fill represents the observation of SKS-SKKS waveforms, with red for at least one discrepant pair and yellow for only non-discrepant recordings. White triangles display sites at which no SKS-SKKS pairs were observed. C: Distribution of earthquakes that yielded at least one discrepant (red) or non-discrepant (yellow) SKS-SKKS pair.

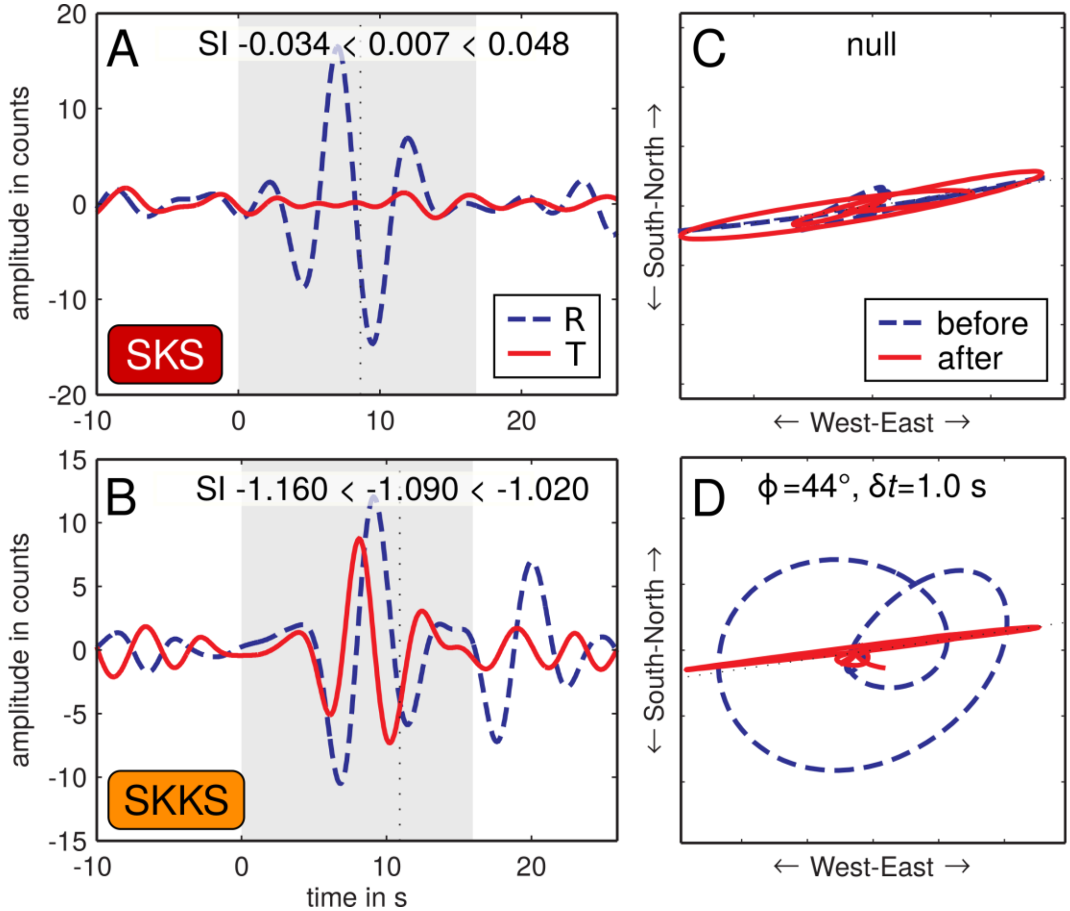

Figure 2. A and B: Original (uncorrected) radial (R, blue dashed) and transverse (T, solid red) component seismograms at station PVF for SKS (top) and SKKS (bottom) of the same event at 25/07/2016. At the top the splitting intensity (SI) value along with its

DOI:10.1130/G45514.1

uncertainty (95% confidence interval) is shown. C and D: Particle motions before (blue dashed) and after (solid red) correcting the splitting using the Silver and Chan (1991) method. Splitting parameters ϕ and δt or null are indicated at the top of each panel.

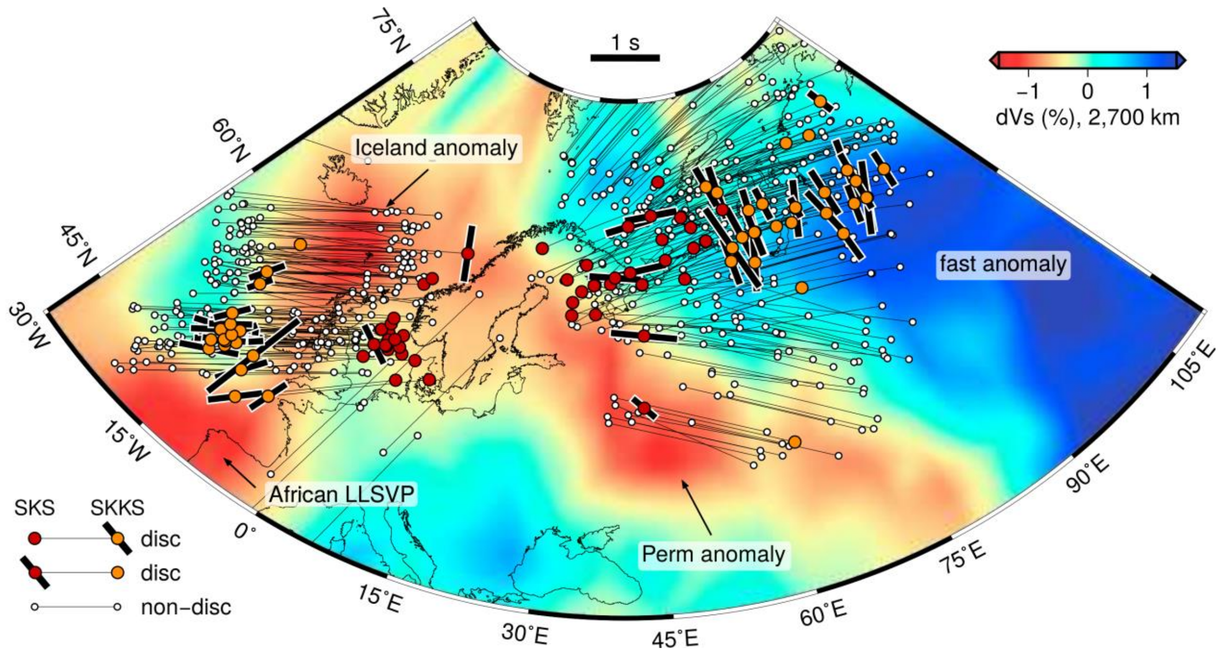

Figure 3. D″ pierce points of SKS-SKKS pairs calculated with the tauP toolkit based on the iasp91 earth model (Crotwell et al., 1999) atop the GyPSuM global v_S tomography model at 2,700 km depth (Simmons et al., 2010). Discrepant pairs are marked with red (SKS) and orange (SKKS) dots, the split phase is indicated with a black bar oriented in the direction of ϕ and scaled by δt (as observed at the station). Related pierce points are connected by thin black lines. White dots indicate non-discrepant pairs.

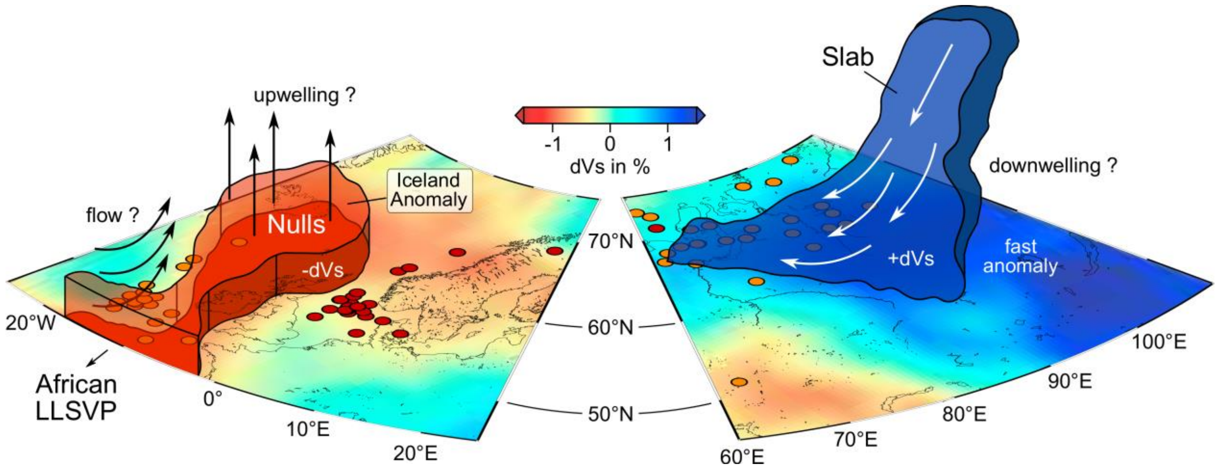

Figure 4. Interpretation of our findings based on two of the most plausible sources of D″ anisotropy. Beneath the Atlantic, nearly horizontal mantle flow potentially induces anisotropy along the northern extensions of the African Large Low Shear Velocity Province (LLSVP) toward the Iceland Anomaly. Absence of splitting (null) is observed for the majority of measurements that correspond to pierce points located within the Iceland Anomaly and potentially indicates vertical flow. Beneath Siberia downwelling (colder than average) material of a subducted slab imprints anisotropy in a widespread area atop the core-mantle boundary.

[1]GSA Data Repository item **2019049**, Table DR1 (individual splitting measurements) and Figures DR2-DR14 (stereoplots, examples of SKS-SKKS and sSKS splitting, Fresnel zone estimates, event statistics, two record sections, map of split-split pairs, map of ΔSI, geological units, model agreement for fast and slow v_S, overview LMM studies), is available online at **http://www.geosociety.org/datarepository/2019/**, or on request from editing@geosociety.org.